2002

Modeling the Effects of Ion Association on Alternating Current Impedance of Solid Polymer Electrolytes

Changqing Lin
University of South Carolina - Columbia

Ralph E. White
University of South Carolina - Columbia, white@cec.sc.edu

Harry J. Ploehn
University of South Carolina - Columbia, ploehn@cec.sc.edu

Publication Info

Journal of the Electrochemical Society, 2002, pages E242-E251.

Publisher's link: http://dx.doi.org/10.1149/1.1480018
DOI: 10.1149/1.1480018

Journal of The Electrochemical Society, **149** (7) E242-E251 (2002)
0013-4651/2002/149(7)/E242/10/$7.00 © The Electrochemical Society, Inc.

Modeling the Effects of Ion Association on Alternating Current Impedance of Solid Polymer Electrolytes

Changqing Lin,*,[a] Ralph E. White, and Harry J. Ploehn[z]**

Department of Chemical Engineering, University of South Carolina, Columbia, South Carolina 29208, USA

This work presents a rigorous continuum model describing the transport of ions and associated ion pairs in solid polymer electrolytes subjected to small amplitude alternating current (ac) excitation. The model treats ion association as a reversible reaction among ions and ion pairs. Dimensionless governing equations are developed from component mass balances, flux equations based on dilute solution theory, and the Poisson equation. Assuming reversible electrode reactions and electroneutrality, the model equations have an analytical solution. Further simplifications are possible in limiting cases (weak and strong association, zero and infinite frequency excitation), giving expressions consistent with previously published models. We use the model to explore the effect of association/dissociation reaction rates, ion pair diffusivity, and fractional dissociation on ac impedance behavior. We present a scheme for establishing component diffusivities and fractional dissociation from independent experimental data for lithium perchlorate in poly(ethylene oxide). With no additional adjusted parameters, satisfactory agreement exists between calculated and experimental ac impedance data.
 [DOI: 10.1149/1.1480018]

Manuscript submitted July 26, 2001; revised manuscript received Janaury 10, 2002. Available electronically May 9, 2002.

Considerable experimental evidence indicates that ion association occurs in many solid polymer electrolytes. For example, conductivity measurements and spectroscopy data provide evidence for ion association in $LiCF_3SO_3$/polyethylene oxide (PEO),[1,2] $LiClO_4$/PEO,[2] $LiCF_3SO_3$/PPG,[3] $NaBF_4$/PEO,[4] and $NaBH_4$/PEO.[4] However, the mathematical models used to extract transport properties from the data do not generally account for ion association. Instead, transport properties are interpreted in the context of the usual strong electrolyte model.[5] The impact of this assumption may differ from one technique to another, so accurate, consistent values of ionic diffusion coefficients and transference numbers may be difficult to obtain. Specifically, small signal ac and dc conductance measurements will not yield accurate values of transport properties if ion association changes the number and mobility of charge carriers. Pulsed-field-gradient nuclear magnetic resonance (NMR) spectroscopy[6] only provides values of transport properties representing averages over atoms as free ions and ion pairs.

Recognizing this limitation, models of battery cell performance[7] rely on empirical correlations of conductivity data (again, interpreted in the context of strong electrolyte) rather than a more fundamental description. The empirical approach provides the basic data needed to engineer a particular device, but nothing more, no deeper understanding of transport mechanisms, nor any basis for extrapolating to other conditions. Furthermore, the empirical approach is labor-intensive, necessitating many measurements to describe, for example, the complete temperature- and concentration-dependence of ionic conductivity.

More sophisticated models of ion transport may be able to address these concerns. In particular, models of ion transport in polymer electrolytes should account for ion association. By reducing the number of experiments needed to characterize electrolyte conductivity, such a model may serve as a phenomenological aid. Moreover, ion association models may provide greater insight into the fundamental mechanisms of ion transport in polymer electrolytes.

To this end, our previous work[8] describes a rigorous theoretical analysis of the effect of ion association on direct current (dc) conductivity, general current-potential behavior, and limiting current density in solid polymer electrolytes. The predictions of the model highlight the effects of the relative diffusion coefficients and dimensionless association constant on concentration distributions of simple ions and ion pairs, the limiting current density, and the potential drop required to drive a specified current density. The qualitative trends of these predictions are in accord with experimental observations. However, no single dc measurement (*e.g.*, conductivity, current *vs.* potential, or limiting current density), analyzed in conjunction with the dc model, can be used to quantify the extent of ion association. Additional experimental data are needed to establish values of all of the model's dimensionless parameters.

Other obvious sources of data are alternating current (ac) impedance experiments. Much effort has been devoted to developing models of ion transport under ac excitation. The early work of MacDonald[9-12] accounted for ion-ion interactions via the Poisson equation. Ultimately, this model[12] was extended to include the effects of ion association modeled as an equilibrium reaction between ions and neutral, immobile ion pairs. The ac transport model of Pollard and Comte[13] employed concentrated solution theory under the assumption of electroneutrality. This analysis considered not only ion association, but also the existence of a second nonconducting phase in the electrolyte. However, the results were only discussed under the special situation when the ion-pairing reaction was in equilibrium and the total reaction rate was set to zero. Likewise, the model of Lorimer *et al.*[14] employs concentrated solution theory and electroneutrality as well as electrode kinetics governed by the Butler-Volmer equation, but it assumes that all species have the same diffusion coefficient. Franceschetti *et al.*[15] modeled ac ion transport in both supported and unsupported electrolytes in a thin layer cell for completely dissociated salt. They compared results based on the electroneutrality assumption with those of MacDonald[9] using the Poisson equation. The Franceschetti *et al.* model has a straightforward development and gives a clear physical picture but does not treat ion association.

A complete, rigorous model of ac impedance that considers both ion association and ion-ion interaction via the Poisson equation has not been published. Even models assuming electroneutrality do not treat ion association fully and in depth. In this work, we develop a model to describe ion transport in solid polymer electrolytes under small signal ac excitation. The model formulation includes the Poisson equation, although we report results only for conditions of electroneutrality. We investigate the effects of ion association on species transport processes in thin layers of polymer electrolyte. The model yields predictions of electrolyte impedance which are compared with experimental data. We show how this model may be used in conjunction with ac impedance experiments to characterize ion association of lithium salt in polymer electrolytes.

Transport Model

Assumptions.—Our objective is a continuum model for transport and reaction of ionic species in polymer electrolytes under ac excitation. We invoke several simplifying assumptions.

* Electrochemical Society Active Members.
** Electrochemical Society Fellow.
[a] Present address: Microcell, 6003 Chapel Hill Road, Suite 153, Raleigh, NC 27607, USA.
[z] E-mail: ploehn@engr.sc.edu

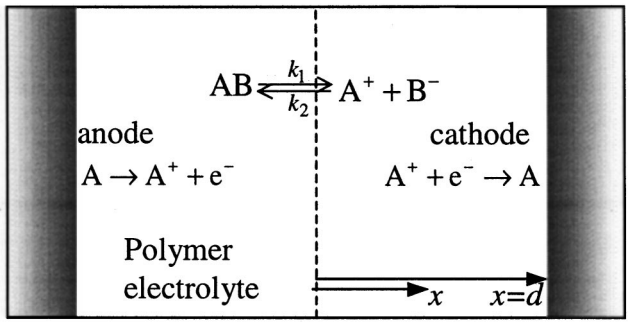

Figure 1. Schematic diagram of a solid polymer electrolyte phase ($-d < x < d$) bounded by planar cathode and anodes.

1. The domains of the electrode and electrolyte phases (Fig. 1) have planar symmetry with no variations in the lateral dimensions. The origin $x = 0$ is located at the center of the electrolyte, and the electrolyte-cathode interface is at $x = d$.

2. The electrolyte phase consists of an immobile, nonreactive polymer, univalent cations (A^+), univalent anions (B^-), and ion pairs (AB). No supporting salts are present. We do not consider higher-order aggregates (triplets, etc.).

3. The polymer concentration is constant. The concentrations of A^+, B^-, and AB, denoted by c_+, c_-, and c_p, vary with position and time. The total salt concentration, c_s, is a known, constant parameter.

4. Dilute solution theory[16] describes the transport of A^+, B^-, and AB. The species' diffusion coefficients are defined as effective binary coefficients and are constant.

5. Ions and ion pairs are not assumed to be in equilibrium. Ion pairs dissociate according to

$$AB \underset{k_2}{\overset{k_1}{\rightleftarrows}} A^+ + B^- \qquad [1]$$

with k_1 and k_2 denoting the forward and backward reaction rates, respectively. The molar production rates of A^+, B^-, and AB are related by

$$R_+ = R_- = -R_p = k_1 c_p - k_2 c_+ c_- \qquad [2]$$

based on the assumption of univalent stoichiometry.

6. Only cations are electroactive at the electrolyte-electrode interfaces. We have

$$A^+ + e^- \rightarrow A \qquad [3]$$

at the cathode located at $x = d$, and the opposite reaction at the anode located at $x = -d$. The net rate of generation of A^+ due to interfacial reactions (superscript σ) is denoted as R^{σ}_+. The corresponding interfacial reaction rates for anions and ion pairs are zero.

7. The rates of interfacial reactions are fast compared to all other processes in the system. We do not treat the case of finite electrode kinetics here.

Transport equations.—The Appendix presents a complete development of governing equations describing the transport of A^+, B^-, and AB in a polymer electrolyte subjected to small amplitude alternating current excitation. In brief, the development begins with expressions for the component mass balances and fluxes (Eq. A-1 to A-3), the Poisson equation (A-4), and flux boundary conditions derived from component jump mass balances.[17] (The term ''jumping mass balance'' refers to a specialized form of the differential mass balance valid only at the discontinuous interface between two phases.) Since the cation flux is proportional to the specified current density, we do not need to specify a kinetic rate expression for cation reduction at the cathode. The equations are linearized for small amplitude ac excitations. After expressing the concentration and potential profiles in terms of steady-state and time-dependent parts,[15] we show that the steady-state solution satisfies the equilibrium conditions that one expects under the assumptions of electroneutrality and zero direct current. The equations for the time-dependent contributions to the concentration and potential profiles are simplified and made dimensionless by defining the dimensionless variables and groups as shown in Table I, yielding

Table I. Dimensionless variables and groups.

Variables	Physical meaning
$X \equiv x/d$	Dimensionless position
$C_{i1} \equiv c_{+1}/c_s$	Dimensionless time-dependent concentration of component $i = +, -, p$
$\Phi_1 \equiv F\phi_1/RT$	Dimensionless time-dependent potential
$\Omega \equiv \omega d^2/D_s$	Dimensionless frequency
$\overline{\Delta E} = F\Delta E/RT$	Dimensionless potential drop across the cell
$\overline{Z} = ZF^2D_+c_s/RTd$	Dimensionless impedance
Groups	**Physical meaning**
$D_s \equiv \frac{2D_+D_-}{D_+ + D_-}$	Salt diffusion coefficient
$t_i = \frac{D_i}{D_+ + D_-}$	Transference number for ions $i = +, -$
$\Pi_{k_1} \equiv k_1 d^2/D_s$	Dimensionless reaction rate for ion pair dissociation
$\Pi_{k_2} \equiv k_2 c_s d^2/D_s$	Dimensionless reaction rate for ion pair formation
$\Pi_d \equiv \Pi_{k_1}/\Pi_{k_2}$	Dimensionless equilibrium dissociation constant $[\Pi_d = \alpha^2/(1-\alpha)]$
$\alpha \equiv c_{+0}/c_s = c_{-0}/c_s$	Salt degree of dissociation (related to Π_d in Eq. A-18)
$\Pi_p \equiv D_p/D_s$	Dimensionless ion pair diffusivity relative to that of salt
$\Pi_I \equiv I_1 d/FD_+c_s$	Dimensionless time-dependent current density
$\kappa = \sqrt{2F^2c_s/\varepsilon RT}$	Reciprocal Debye length

$$\frac{\partial^2 C_{+1}}{\partial X^2} = (2\alpha\Pi_{k_2} + i\Omega)C_{+1} - \Pi_{k_1}C_{p1} \qquad [4]$$

$$\frac{\partial^2 C_{p1}}{\partial X^2} = \frac{-2\alpha\Pi_{k_2}C_{+1}}{\Pi_p} + \frac{1}{\Pi_p}(i\Omega + \Pi_{k_1})C_{p1} \qquad [5]$$

with the boundary conditions

$$X = 1: \quad \frac{\partial C_{+1}}{\partial X} = -\frac{\Pi_I}{2} \qquad [6]$$

$$X = 1: \quad \frac{\partial C_{p1}}{\partial X} = 0 \qquad [7]$$

$$X = 0: \quad C_{+1} = 0, \quad C_{p1} = 0 \qquad [8]$$

Equations 4-8 can be solved to obtain the concentration profiles (see Appendix)

Table II. Eigenvalues and eigenvector elements in several limiting cases.

Special cases	Λ_1	Λ_2	u_1	u_2
$\Pi_{k_2} = 0$	$i\Omega$	$\frac{(i\Omega + \Pi_{k_1})}{\Pi_p}$	$\frac{i\Omega(1 - \Pi_p) + \Pi_{k_1}}{2\alpha\Pi_{k_2}}$	0
$\Pi_{k_1} \to 0$	$i\Omega + 2\alpha\Pi_{k_2}$	$\frac{i\Omega}{\Pi_p}$	0	$\frac{i\Omega(1 - \Pi_p)}{2\alpha\Pi_{k_2}} - \Pi_p$
$\Omega \to \infty$	$i\Omega \to \infty$	$\frac{i\Omega}{\Pi_p} \to \infty$	0	$\frac{i\Omega(1 - \Pi_p)}{2\alpha\Pi_{k_2}} \to \infty$
$\Omega \to 0$	$\frac{\Pi_{k_1}}{\Pi_p} + 2\alpha\Pi_{k_2}$	$\Lambda_2 \to 0$	$-\Pi_p$	$\frac{\Pi_{k_1}}{2\alpha\Pi_{k_2}}$

$$C_{+1} = -\frac{u_1}{u_1 - u_2}\frac{1}{\sqrt{\Lambda_1}\cosh(\sqrt{\Lambda_1})}\frac{\Pi_I}{2}\sinh(\sqrt{\Lambda_1}X) + \frac{u_2}{u_1 - u_2}\frac{1}{\sqrt{\Lambda_2}\cosh(\sqrt{\Lambda_2})}\frac{\Pi_I}{2}\sinh(\sqrt{\Lambda_2}X) \quad [9]$$

and

$$C_{p1} = -\frac{1}{u_1 - u_2}\frac{1}{\sqrt{\Lambda_1}\cosh(\sqrt{\Lambda_1})}\frac{\Pi_I}{2}\sinh(\sqrt{\Lambda_1}X) + \frac{1}{u_1 - u_2}\frac{1}{\sqrt{\Lambda_2}\cosh(\sqrt{\Lambda_2})}\frac{\Pi_I}{2}\sinh(\sqrt{\Lambda_2}X) \quad [10]$$

with eigenvalues and eigenvector elements specified in Eq. A-44 to A-47.

Cell impedance.—The cell impedance is given by

$$Z(\omega) = \frac{\Delta E}{I_1} = \frac{\Delta E_1 + \Delta E_2}{I_1} \quad [11]$$

As discussed by Franceschetti *et al.*,[15] the potential drop across the cell includes contributions due to diffusion and migration (ΔE_1) and electrode reactions (ΔE_2). The first part can be found from

$$\Delta E_1 = \phi_1(-d) - \phi_1(d) \quad [12]$$

ΔE_2 represents the electrode overpotential and depends on electrode kinetics. If we assume reversible electrode kinetics, the Nernst equation gives ΔE_2 which, after linearization, is

$$\Delta E_2 = \frac{RT}{Fc_{+0}}[c_{+1}(-d) - c_{+1}(d)] \quad [13]$$

In terms of the dimensionless variables defined in Table I, Eq. 11-13 become

$$\overline{Z}(\Omega) = \frac{\overline{\Delta E}}{\Pi_I} = \frac{\overline{\Delta E_1} + \overline{\Delta E_2}}{\Pi_I} \quad [14]$$

$$\overline{\Delta E_1} = \Phi_1(-1) - \Phi_1(1) \quad [15]$$

$$\overline{\Delta E_2} = \frac{1}{\alpha}[C_{+1}(-1) - C_{+1}(1)] = -\frac{2}{\alpha}C_{+1}(1) \quad [16]$$

From the solutions obtained in the Appendix (Eq. A-57 and A-67), the total potential drop and cell impedance are

$$\overline{\Delta E} = 2t_-\left[\frac{u_1}{u_1 - u_2}\frac{1}{\sqrt{\Lambda_1}}\tanh(\sqrt{\Lambda_1}) - \frac{u_2}{u_1 - u_2}\frac{1}{\sqrt{\Lambda_2}}\tanh(\sqrt{\Lambda_2})\right]\Pi_I + \frac{2t_+\Pi_I}{\alpha} \quad [17]$$

and

$$\overline{Z}(\Omega) = \frac{2t_-}{\alpha}\left[\frac{u_1}{u_1 - u_2}\frac{1}{\sqrt{\Lambda_1}}\tanh(\sqrt{\Lambda_1}) - \frac{u_2}{u_1 - u_2}\frac{1}{\sqrt{\Lambda_2}}\tanh(\sqrt{\Lambda_2})\right] + \frac{2t_+}{\alpha} \quad [18]$$

Equations A-44 to A-47 express the eigenvalues (Λ_1 and Λ_2) and eigenvector elements (u_1 and u_2) in terms of the key dimensionless groups, Π_{k_1}, Π_{k_2}, and Π_p.

Results and Discussion

In this section, we first present simplified expressions for ac impedance in some special limiting cases. Next, we consider the effects of ion association on ac impedance under general conditions. Finally, we show how the model may be used in conjunction with experiments to characterize ion association in solid polymer electrolytes.

Limiting cases.—It is instructive to consider simplified expressions for cell impedance in a variety of limiting cases, including complete dissociation ($\Pi_{k_2} \to 0$), strong association ($\Pi_{k_1} \to 0$), zero frequency ($\Omega \to 0$), and infinite frequency ($\Omega \to \infty$). The eigenvalues and eigenvector elements for these limiting cases, derived from Eq. A-44 to A-47, are summarized in Table II.

Complete dissociation.—Substituting the eigenvalues for this case ($\Pi_{k_2} \to 0$, $\alpha \to 1$) from Table II into Eq. 18 produces the cell impedance for the case of complete ion dissociation

$$\overline{Z}(\Omega) = 2\left[t_+ + \frac{t_-}{\sqrt{i\Omega}}\tanh(\sqrt{i\Omega})\right] \quad [19]$$

The dimensional form is

$$Z(\omega) = \frac{2dRT}{F^2c_s}\left[\frac{1}{(D_+ + D_-)} + \frac{2t_-^2}{d\sqrt{i\omega D_s}}\tanh\left(\sqrt{\frac{i\omega}{D_s}}d\right)\right] \quad [20]$$

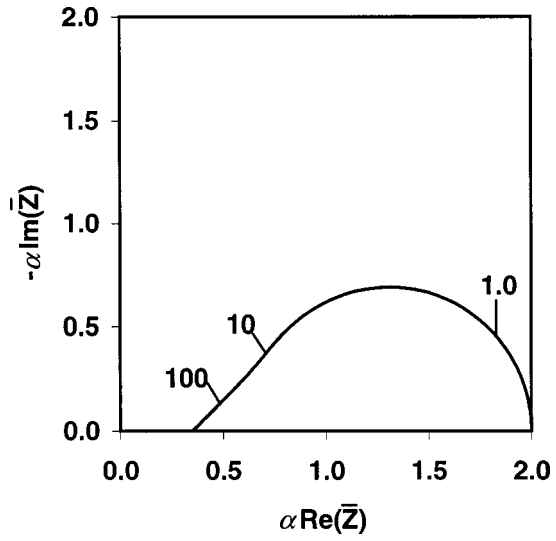

Figure 2. Nyquist plot of the impedance response (dimensionless, multiplied by fractional dissociation, α) for the limiting cases of complete dissociation (Eq. 19, $\alpha = 1$) and strong association (Eq. 21, $\alpha = 0.01$). Other parameters for the strong association case include $t_+ = 0.175$, $t_- = 0.825$, and Π_p=0.5, 1.0, and 2.0. Dimensionless frequencies for the complete dissociation case are also shown at selected points.

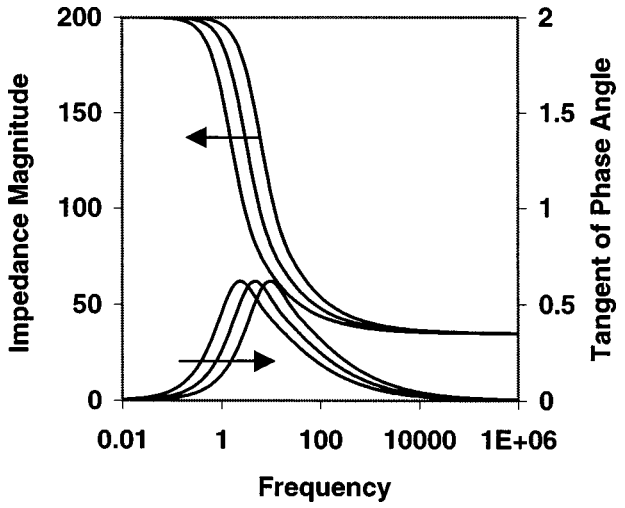

Figure 3. Bode plot of the impedance magnitude (dimensionless, left) and phase angle (right) for the strong association limiting case (Eq. 21, $\alpha = 0.01$). Other parameters include $t_+ = 0.175$, $t_- = 0.825$, and $\Pi_p = 0.5$, 1.0, and 2.0 (left, center, and right curves in each set of three).

These expressions are in accord with results obtained previously.[13-15] The Nyquist plot of $\overline{Z}(\Omega)$, shown in Fig. 2 (with $\alpha = 1$), manifests the classic Warburg impedance behavior at high frequencies. The curvature at low frequencies becomes important when the characteristic diffusion length ($\sqrt{D_s/\omega}$) is comparable to the cell thickness ($2d$).

Strong association.—Here, we have $\Pi_{k_1} \to 0$. Substituting the eigenvalues from Table II into Eq. 18 gives

$$\overline{Z}(\Omega) = \frac{2}{\alpha}\left[t_+ + \frac{t_-}{\sqrt{i\Omega/\Pi_p}}\tanh(\sqrt{i\Omega/\Pi_p})\right] \qquad [21]$$

or

$$Z(\omega) = \frac{2dRT}{F^2 c_s \alpha}\left[\frac{2t_-^2}{D_s\sqrt{\frac{i\omega}{D_p}}d}\tanh\left(\sqrt{\frac{i\omega}{D_p}}d\right) + \frac{1}{(D_+ + D_-)}\right] \qquad [22]$$

in dimensional form. The impedance has the same form as in the complete dissociation case, but it now depends on the ion pair diffusivity and is inversely proportional to the fractional dissociation α. With regard to the general shape, the Nyquist plot of $\alpha\overline{Z}(\Omega)$ for strong association (Fig. 2) is indistinguishable from that for complete dissociation (Eq. 19). Varying the value of Π_p shifts the impedance behavior along the frequency axis without changing the shape of the response in the Nyquist plot. However, the corresponding Bode plot (Fig. 3) shows that increasing the value of Π_p shifts the relaxation of the impedance response to higher frequency.

These results have a clear physical interpretation. Concentration polarization produces the high impedance magnitude seen at low frequency (Fig. 3). Relaxation of the response occurs when diffusion/migration processes cannot keep up with the oscillating applied current, leading to decreasing concentration polarization and impedance. The impedance relaxes to a purely ohmic resistance at high frequency. In the strong association limit dominated by ion pairs, increasing the relative ion pair mobility enables concentration polarization to occur at higher frequencies. Thus we see the impedance relaxation shift to the right in Fig. 3 as Π_p increases.

High frequency limit.—In this case, using the results in Table II, Eq. 18 becomes

$$\overline{Z}_\infty = \lim_{\Omega\to\infty}\left[\frac{2t_-}{\alpha\sqrt{i\Omega/\Pi_p}}\tanh(\sqrt{i\Omega/\Pi_p}) + \frac{2t_+}{\alpha}\right] = \frac{2t_+}{\alpha} \qquad [23]$$

or, in dimensional form

$$Z_\infty = \frac{2dRT}{F^2 c_s \alpha (D_+ + D_-)} \qquad [24]$$

The impedance in the high frequency limit is independent of Π_{k_1}, Π_{k_2}, and Π_p and only varies with D_+, D_-, c_s, and α. If three of these parameters are known, a high-frequency impedance measurement can be used to determine the fourth. Specifically, with ion diffusivities from independent measurements, Eq. 24 can be used to determine α from Z_∞. Conversely, if α can be estimated from dc conductivity data, Z_∞ and Eq. 24 determine $(D_+ + D_-)$.

Zero frequency limit.—Again, using the results in Table II, Eq. 18 becomes

$$\overline{Z}_0 = \frac{2t_-}{\alpha}\left[\frac{2\alpha\Pi_{k_2}}{2\alpha\Pi_{k_2} + \Pi_{k_1}/\Pi_p}\frac{\tanh(\sqrt{\Pi_{k_1}/\Pi_p + 2\alpha\Pi_{k_2}})}{\sqrt{\Pi_{k_1}/\Pi_p + 2\alpha\Pi_{k_2}}} + \frac{\Pi_{k_1}/\Pi_p}{2\alpha\Pi_{k_2} + \Pi_{k_1}/\Pi_p}\right] + \frac{2t_+}{\alpha} \qquad [25]$$

In the case of complete dissociation ($\Pi_{k_2} \to 0$, $\alpha \to 1$), Eq. 25 reduces to

$$\overline{Z}_0 = 2 \quad \text{or} \quad Z_0 = \frac{2dRT}{F^2 c_s D_+} \qquad [26]$$

in agreement with previous models for completely dissociated salt.[15] The impedance in the dc limit for completely dissociated salt depends only on the cation diffusion coefficient.

For finite levels of ion association, if the rates of ion pair dissociation and association are fast compared to $1/\omega$ as $\omega \to 0$, then Reaction 1 (Eq. 1) is at equilibrium, and we have

$$\frac{\tanh(\sqrt{\Pi_{k_1}/\Pi_p + 2\alpha\Pi_{k_2}})}{\sqrt{\Pi_{k_1}/\Pi_p + 2\alpha\Pi_{k_2}}} \to 0 \qquad [27]$$

Equation 25 simplifies to

$$\overline{Z_0} = \frac{2}{\alpha}\left[\frac{t_-\Pi_d}{(2\alpha\Pi_p + \Pi_d)} + t_+\right] = 2\left[\frac{t_-}{2(1-\alpha)\Pi_p + \alpha} + \frac{t_+}{\alpha}\right] \qquad [28]$$

or, in dimensional form

$$Z_0 = \frac{2RTd}{F^2 D_+ c_s}\left\{\frac{t_-}{[2(1-\alpha)D_p/D_s + \alpha]} + \frac{t_+}{\alpha}\right\} \qquad [29]$$

With measurement of Z_0 and independent knowledge of ionic diffusivities, Eq. 29 provides a useful relationship between α and D_p. Furthermore, Eq. 28 and 29 also represent exact expressions for direct current conductivity in the limit of small current density. We were unable to obtain a corresponding analytical expression from our previous dc polarization model.[8] After appropriate translation of dimensionless groups, we find that the zero frequency conductivity derived from Eq. 28 agrees perfectly with the numerical dc conductivity results shown in Fig. 9 of Ref. 8.

Further limiting cases derived from Eq. 29 are also noteworthy. When ion pairs are immobile ($D_p = 0$), Z_0 becomes

$$Z_0 = \frac{2RTd}{F^2 D_+ c_s \alpha} \qquad [30]$$

This result reduces to Eq. 26 for completely dissociated salt ($\alpha \to 1$). In the opposite limit of complete association of ions as immobile ion pairs ($\alpha \to 0$), the zero frequency impedance becomes infinite, as one would expect. Finally, when $\alpha > 0$ and $D_p \gg D_s$, Eq. 29 becomes

$$Z_0 = \frac{2RTdt_+}{F^2 D_+ c_s \alpha} = \frac{2RTd}{F^2(D_+ + D_-)c_s\alpha} \qquad [31]$$

General trends .—This section provides an overview of the effects of ion association on general trends in ac impedance behavior, focusing primarily on variations of dissociation and association reaction rates (Π_{k_1}, Π_{k_2}), ion pair relative diffusivity (Π_p), and salt fractional dissociation (α).

Association/dissociation reaction rates.—With respect to the association and dissociation reactions shown in Eq. 1, we generally assume that the reaction rates are fast compared to both diffusion and the period of the ac oscillation (*i.e.*, equilibrium among ion and ion pairs). Figure 4 shows that as long as the dimensionless rate constants are large (keeping the ratio $\Pi_{k_1}/\Pi_{k_2} \equiv \Pi_d$ and thus α constant), the impedance response is independent of these rates. However, if we decrease the association and dissociation rate constants, an unusual peak appears in the impedance magnitude. This peak grows and shifts to lower frequency as the rate constants decrease. Rationalization of this feature as an artifact of the model or a real physical phenomenon will require further investigation. In the present work, we avoid the issue by assuming equilibrium of Eq. 1.

Ion pair diffusivity.—The ion pair diffusivity D_p should not be confused with the salt diffusivity D_s commonly employed as a mean value of cation and anion diffusivities. As discussed previously,[8] the ion pair diffusivity may be greater than that of cations or anions due to attractive interactions between free ions and the polymer electrolyte. Thus, $\Pi_p \equiv D_p/D_s$ may be either larger or smaller than 1.0. In the context of lithium systems, the diffusivity of Li+ may be reduced due to coordination with ether oxygens in PEO. If, for example, $D_+ = 0.5D_-$ and $D_p = D_-$, one can easily show that $\Pi_p = 1.5$.

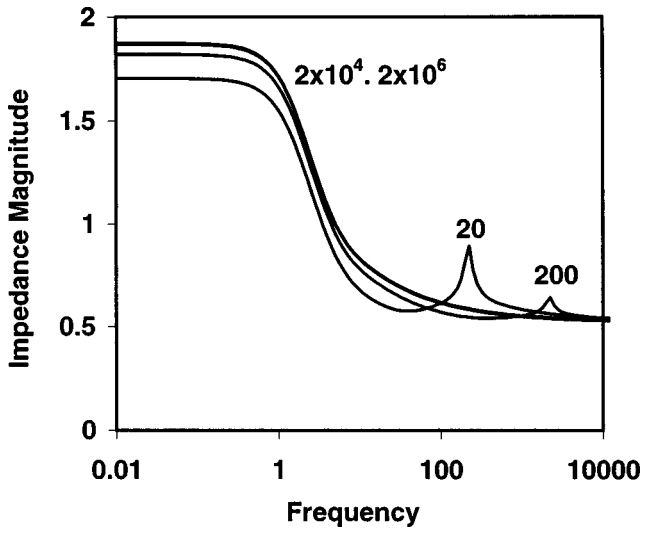

Figure 4. Effect of association/dissociation reaction rates (Π_{k_1} values shown on the plot, $\Pi_{k_2} = \Pi_{k_1}/1.33$ or $\alpha = 0.67$), on the dimensionless impedance magnitude. Other parameters include $t_+ = 0.175$, $t_- = 0.825$, and $\Pi_p = 0.83$.

Figure 5 shows the Nyquist plot of the ac impedance calculated from Eq. 18 for the indicated values of Π_p. We have chosen large values for Π_{k_1} and Π_{k_2} so that diffusion processes, rather than the homogeneous reaction rates, dominate the response. In general, both the real and imaginary components of the impedance decrease with increasing Π_p values. The trend at low frequencies is similar to that seen previously[8] for dc polarization. In effect, ion pairs provide a parallel mechanism for transporting cations; increasing Π_p promotes this mechanism, reduces concentration polarization, and therefore decreases the impedance (at fixed frequency and fractional dissocia-

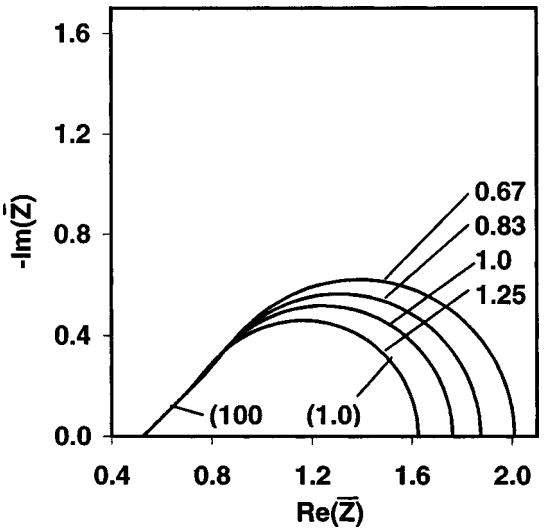

Figure 5. Effect of ion pair diffusivity (Π_p values shown on the plot), on the dimensionless impedance (Nyquist plot). Other parameters include with $t_+ = 0.175$, $t_- = 0.825$, $\Pi_{k_1} = 2 \times 10^6$, $\Pi_{k_2} = 1.5 \times 10^6$, and $\alpha = 0.67$. Dimensionless frequencies (shown in parentheses) for the $\Pi_p = 1.25$ case are also shown at selected points.

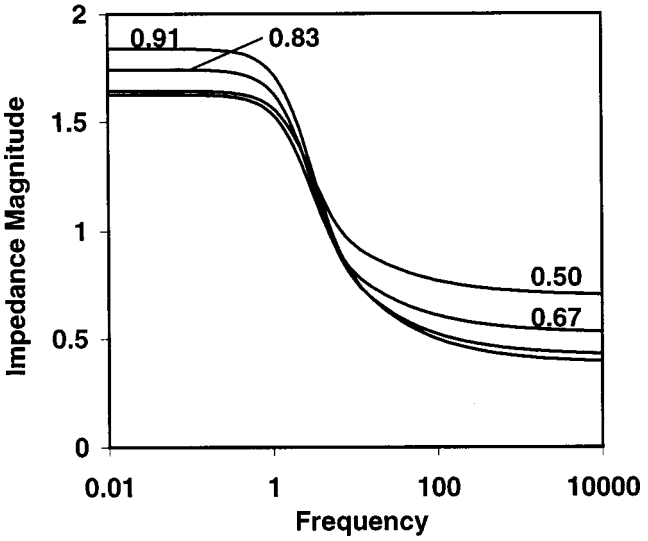

Figure 6. Effect of salt fractional dissociation (α values shown on a Bode plot) on dimensionless impedance magnitude for $\Pi_p = 1.25$. Other parameters as in Fig. 5.

tion). The corresponding Bode plot (not shown) indicates that impedance depends only weakly on Π_p at moderate to high frequencies for which concentration polarization is unimportant. The convergence of all curves at high frequency is also in accord with the limiting case result, Eq. 23.

Fractional dissociation.—Figure 6 ($\Pi_p = 1.25$, Bode plot) and Fig. 7 ($\Pi_p = 0.67$, Nyquist plot) explore the effect of varying the fractional dissociation while holding constant the ion pair diffusivity. As the fractional dissociation increases, more charge carriers are produced, and so the impedance magnitude at high frequencies (Fig. 6) decreases. Since diffusion is unimportant at high frequencies, the impedance is independent of Π_p as also seen in Fig. 5.

At low frequencies, the dependence of impedance on Π_p and α is consistent with the dc conductivity results reported previously.[8] In the previous work (Fig. 9 of Ref. 8), we found a maximum in the

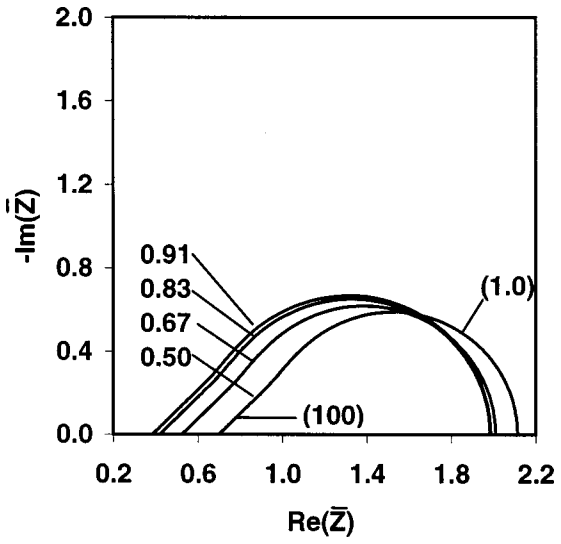

Figure 7. Effect of salt fractional dissociation (α values shown on the Nyquist plot) on dimensionless impedance magnitude for $\Pi_p = 0.67$. Dimensionless frequencies (shown in parentheses) for the $\alpha = 0.50$ case are also shown at selected points. Other parameters as in Fig. 5.

molar conductivity with varying fractional association. This corresponds to the impedance minimum with varying α seen in the low frequency data in Fig. 6 and 7. As fractional dissociation decreases from $\alpha = 1$, the low frequency impedance initially decreases due to the formation of ion pairs that are more mobile than simple ions. However, further decrease of α ultimately binds up all of the charge-carrying ions into ion pairs, so the low frequency impedance goes through a minimum and then increases. We observe this trend for ion pairs that are more mobile (Fig. 6, $\Pi_p = 1.25$) as well as less mobile (Fig. 7, $\Pi_p = 0.67$) than the salt average. In these cases, the ion transference numbers are such that the ion pair diffusivity is significantly greater than that of at least one of the simple ions. A more complete view of the variations of low-frequency impedance with Π_p and α can be inferred from the discussion of Fig. 9 in Ref. 8, recognizing the reciprocal relationship between impedance magnitude and conductivity.

Comparison with experimental data.— As mentioned before, ion association complicates the determination of electrolyte transport properties. Accurate, consistent values for ion and ion pair diffusivities and fractional dissociation may be difficult to obtain from NMR or conductivity measurements.[5] ac impedance may offer a solution to this problem, either alone or in combination with other measurements. Furthermore, the combination of an appropriate first-principles transport model with a few characterization experiments may be able to reduce the net number of experiments needed to parameterize electrolyte behavior for use in battery cell models.

Four independent experiments are needed to establish values of the three component diffusivities and the fractional dissociation. We can use literature data for $LiClO_4$ in PEO 400 as an illustration. Both ac impedance data[18] and ion self-diffusion coefficients[19] have been published for this system. We assume that values of ion self-diffusion coefficients derived from NMR measurements can be used as mutual diffusion coefficients required in the present transport model. Although ion diffusivities from NMR represent averages for atoms in both simple ion form and associated form,[6] the NMR-derived values should be good approximations if one assumes that ion pairs have diffusivity similar to that of salt. With two diffusivity values (D_+ and D_-) from NMR, we may use the limiting case analytical forms for Z_∞ and Z_0, Eq. 24 and 29, to fix values of the ion pair diffusivity D_p and fractional dissociation α. All other model parameters are known from experimental conditions.

Using the reported[18] impedance values for $LiClO_4$ in PEO 400 (8:1 O/Li ratio) at zero and infinite frequency, we estimate a fractional dissociation $\alpha = 0.56$ and ion pair diffusivity $D_p = 8.88 \times 10^{-12}$ m^2/s ($\Pi_p = 0.77$). Figure 8 compares the model predictions with experimental data (both in dimensional form) over the whole frequency range with no further adjustment of parameters. The agreement between the predicted and measured impedance is satisfactory. Calculated impedance curves for various values of association and dissociation reaction rates show that the value of this parameter is unimportant as long as its value is high.

Conclusions

In this work, we have presented a rigorous continuum model for ion and ion pair transport in polymer electrolytes subjected to ac excitation. After invoking a number of simplifying assumptions, the model equations have analytical solutions that agree with previous models in various limiting cases. The qualitative trends predicted by the model can be rationalized in simple physical terms.

We presented a scheme that uses independent NMR diffusivity data and impedance data in the zero and infinite frequency limits to establish the three component diffusivities and the fractional dissociation of the salt. Despite the significant assumptions of the model, once these four parameters have been fixed, the calculated ac impedance data agree well with experiments with no further adjustment of parameters. Although the values of D_p and α obtained in this way seem reasonable, independent NMR measurements might not be available, or accurate, for this purpose. Certainly our use of

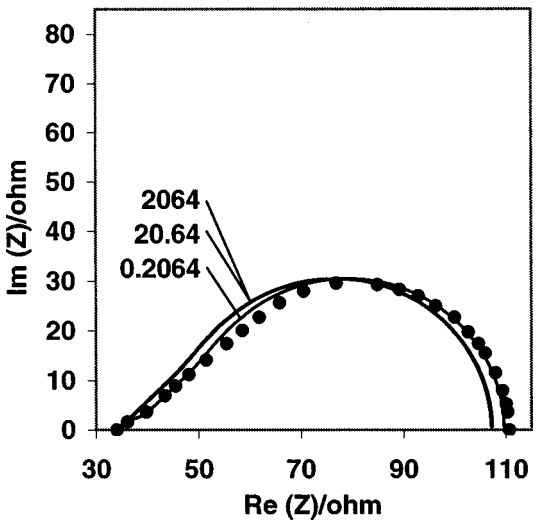

Figure 8. Comparison of calculated (curves) and experimental impedance data[18] (points) for $LiClO_4$ in PEO-400 (8:1 O/Li ratio). Experimental parameters include $T = 403$ K, $2d = 0.3$ mm, $A = 0.5024$ cm^2, and $c_s = 2840$ mol/m^3. NMR experiments[19] provide $D_s = 1.155 \times 10^{-11}$ m^2/s, $t_+ = 0.175$, and $t_- = 0.825$. Model predictions are for various values of k_1 (in s^{-1}) as indicated on the plot.

atom-average NMR data to establish free ion diffusivities fails when the ion pair and free ion diffusivities differ significantly. One way to address this problem would be to account for ion association in the analysis of NMR data in a way consistent with the present association model.

Other schemes relying on combined dc and ac measurements (and avoiding NMR data altogether) may be feasible. For example, the dc model[8] can be used with a measurement of limiting current density to provide one data point involving D_p and α. One ac impedance spectrum provides three additional data points: the zero and infinite frequency limits (for which we have analytical expressions), and the breakpoint frequency (*i.e.*, $\max[-\mathrm{Im}(\overline{Z})]$), for which an analytical expression could also be derived (although we have not done so). In principle, these four data points could be used to establish consistent values for the three component diffusivities and the fractional dissociation without recourse to NMR measurements. Additional dc current-potential and ac impedance data could then be used to assess the quality of the model predictions.

Acknowledgments

We acknowledge the financial support of this work by the U.S. Army Research Office under grant no. DAAH04-96-1-0422.

The University of South Carolina assisted in meeting the publication costs of this article.

Appendix

Transport Equations

General formulation.—Based on assumptions 1-3, the component mass balances can be written as

$$\frac{\partial c_i}{\partial t} = -\frac{\partial N_i}{\partial x} + R_i \qquad [A\text{-}1]$$

with $i = +, -$, and p corresponding to A^+, B^-, and AB, respectively. Dilute solution theory, assumption 4, provides the molar flux expressions

$$N_i = -D_i\frac{\partial c_i}{\partial x} - \frac{D_i Z_i F}{RT} c_i \frac{\partial \phi}{\partial x} \qquad [A\text{-}2]$$

for $i = +, -$, and p. The ion pair valence Z_p is zero. Eliminating molar fluxes between Eq. A-1 and A-2, and substituting the kinetic expression from Eq. 2, gives

$$\frac{\partial c_i}{\partial t} = D_i\frac{\partial^2 c_i}{\partial x^2} + \frac{D_i Z_i F}{RT}\frac{\partial}{\partial x}\left(c_i\frac{\partial \phi}{\partial x}\right) + \nu_i(k_1 c_p - k_2 c_+ c_-) \qquad [A\text{-}3]$$

with the coefficients $\nu_p = -1$ and $\nu_+ = \nu_- = 1$ as indicated by the stoichiometry of Eq. 2. Finally, the Poisson equation

$$\frac{\partial^2 \phi}{\partial x^2} = \frac{F}{\epsilon}\Sigma_i Z_i c_i = \frac{F}{\epsilon}(c_+ - c_-) \qquad [A\text{-}4]$$

relates the potential to the component concentrations.

Boundary conditions must also be specified. At the cathode, the component jump mass balances[17] reduce to

$$x = d: \quad N_+ = R^\sigma_+ \qquad [A\text{-}5]$$

and

$$x = d: \quad N_- = N_p = 0 \qquad [A\text{-}6]$$

as a consequence of assumption 6. Equation A-5 and A-6 provide three of the six required boundary conditions; others are introduced below.

For controlled potential conditions, one specifies the values of potential at the electrode-electrolyte interfaces as well as a kinetic expression for R^σ_+ that depends on the applied potential. The current density in the polymer electrolyte could then be computed from the ionic fluxes through

$$I = -F\sum_i Z_i N_i \qquad [A\text{-}7]$$

Since we wish to consider controlled current conditions, Eq. A-7 may be used as a boundary condition in place of Eq. A-5

$$x = d: \quad N_+ = -\frac{I}{F} \qquad [A\text{-}8]$$

Thus we need not specify the kinetic form of R^σ_+.

In this work, we apply a small amplitude alternating current (ac) excitation to the system

$$I = I_0 + I_1 \exp(i\omega t) \qquad [A\text{-}9]$$

We assume that the excitation has no direct current component ($I_0 = 0$), and that the concentration and potential responses from the small ac excitation can be expressed as the sum of steady-state and time-dependent parts

$$c_i = c_{i0} + c_{i1}\exp(i\omega t) \quad (i = +, -, p) \qquad [A\text{-}10]$$

$$\phi = \phi_0 + \phi_1 \exp(i\omega t) \qquad [A\text{-}11]$$

For small amplitude ac excitation, the nonlinear terms in Eq. A-3 can be linearized so that

$$c_i\frac{\partial \phi}{\partial x} \approx c_{i0}\frac{\partial \phi_0}{\partial x} + \left(c_{i0}\frac{\partial \phi_1}{\partial x} + c_{i1}\frac{\partial \phi_0}{\partial x}\right)\exp(i\omega t) \qquad [A\text{-}12]$$

and

$$k_2 c_+ c_- \approx k_2[c_{+0}c_{-0} + (c_{+0}c_{-1} + c_{+1}c_{-0})\exp(i\omega t)] \qquad [A\text{-}13]$$

Steady-state solution.—After substituting Eq. A-10 to A-13 into Eq. A-3, A-4, A-6, and A-8, the steady-state terms satisfy

$$0 = D_i\frac{\partial^2 c_{i0}}{\partial x^2} + \frac{D_i Z_i F}{RT}\frac{\partial}{\partial x}\left(c_{i0}\frac{\partial \phi_0}{\partial x}\right) + \nu_i(k_1 c_{p0} - k_2 c_{+0}c_{-0}) \qquad [A\text{-}14]$$

and

$$\frac{\partial^2 \phi_0}{\partial x^2} = \frac{F}{\varepsilon}(c_{+0} - c_{-0}) \qquad [A\text{-}15]$$

with boundary conditions

$$x = d: \quad N_i = 0 \qquad [A\text{-}16]$$

In the absence of ion association, no reaction terms would appear in Eq. A-14. In this case, the solution of Eq. A-14 yields ion concentration profiles having the form of Boltzmann distributions. To our knowledge, the diffuse double-layer problem accounting for ion association has not been addressed, nor do we pursue it here. Instead, we assume that the Debye length is very small compared to d, implying electroneutrality

($c_{+0} = c_{-0}$). In this case, Eq. A-15 indicates that the steady-state potential varies linearly with position. Since $I_0 = 0$, we have the steady-state potential ϕ_0 must be independent of position. Hence the migration terms in Eq. A-14 are zero.

It is simple to show[8] that the steady-state ion and ion pair concentrations that satisfy Eq. A-14 and A-16 are independent of position and satisfy equilibrium conditions in the limit of zero current ($I_0 = 0$). An overall mass balance on A atoms in the electrolyte domain

$$\int_0^{2d} (c_{+0} + c_{p0})dx = c_s(2d) \qquad [A\text{-}17]$$

provides another condition; here c_s is the nominal electrolyte salt concentration. We find that

$$c_{+0} = c_{-0} = c_s \frac{\Pi_d}{2}\left[\left(1 + \frac{4}{\Pi_d}\right)^{1/2} - 1\right] \equiv \alpha c_s \qquad [A\text{-}18]$$

and

$$c_{p0} = \frac{c_{+0}^2}{c_s \Pi_d} = c_s\left\{1 + \frac{\Pi_d}{2}\left[1 - \left(1 + \frac{4}{\Pi_d}\right)^{1/2}\right]\right\} \qquad [A\text{-}19]$$

where $\Pi_d \equiv k_1/k_2 c_s$ and α denote the dimensionless equilibrium dissociation constant and fractional degree of dissociation, respectively.

Time-dependent equations.—After substituting Eq. A-10 to A-13 into Eq. A-3, A-4, A-6, and A-8, the time-dependent terms satisfy

$$0 = D_i \frac{\partial^2 c_{i1}}{\partial x^2} + \frac{D_i Z_i F}{RT} c_{i0} \frac{\partial^2 \phi_1}{\partial x^2} + \nu_i[k_1 c_{p1} - k_2(c_{+0}c_{-1} + c_{-0}c_{+1})] - i\omega c_{i1} \qquad [A\text{-}20]$$

and

$$\frac{\partial^2 \phi_1}{\partial x^2} = \frac{F}{\varepsilon}(c_{+1} - c_{-1}) \qquad [A\text{-}21]$$

with flux boundary conditions (from Eq. A-2, A-6, and A-8, linearized in accord with Eq. A-12)

$$x = d: \quad \frac{\partial c_{+1}}{\partial x} + \frac{Z_+ F}{RT} c_{+0} \frac{\partial \phi_1}{\partial x} = -\frac{I_1}{D_+ F} \qquad [A\text{-}22]$$

$$x = d: \quad \frac{\partial c_{-1}}{\partial x} - \frac{Z_- F}{RT} c_{-0} \frac{\partial \phi_1}{\partial x} = 0 \qquad [A\text{-}23]$$

$$x = d: \quad \frac{\partial c_{p1}}{\partial x} = 0 \qquad [A\text{-}24]$$

Using $c_{+0} = c_{-0}$ and Eq. A-21 to eliminate ϕ_1 from Eq. A-20, we have

$$0 = D_i \frac{\partial^2 c_{i1}}{\partial x^2} + \frac{D_i Z_i F^2}{\varepsilon RT} c_{i0}(c_{+1} - c_{-1}) + \nu_i[k_1 c_{p1} - k_2 c_{+0}(c_{+1} + c_{-1})] - i\omega c_{i1} \qquad [A\text{-}25]$$

Equations A-22 and A-23 can be combined to give

$$\frac{\partial(c_{+1} + c_{-1})}{\partial x} = -\frac{I_1}{D_+ F} \qquad [A\text{-}26]$$

Finally, the antisymmetry of the time-dependent concentration profiles[13,15] requires

$$x = 0: \quad c_{i1} = 0 \qquad [A\text{-}27]$$

for each component.

Dimensional analysis.— In terms of the dimensionless variables and groups shown in Table I, Eq. A-21 and A-25 (written for each component) become

$$\frac{\partial^2 \Phi_1}{\partial X^2} = \frac{(\kappa d)^2}{2}(C_{+1} - C_{-1}) \qquad [A\text{-}28]$$

and

$$0 = \frac{\partial^2 C_{+1}}{\partial X^2} + \frac{(\kappa d)^2}{2}\alpha(C_{+1} - C_{-1}) + 2t_-[\Pi_{k_1} C_{p1} - \Pi_{k_2}\alpha(C_{+1} + C_{-1}) - i\Omega C_{+1}] \qquad [A\text{-}29]$$

$$0 = \frac{\partial^2 C_{-1}}{\partial X^2} - \frac{(\kappa d)^2}{2}\alpha(C_{+1} - C_{-1}) + 2t_+[\Pi_{k_1} C_{p1} - \Pi_{k_2}\alpha(C_{+1} + C_{-1}) - i\Omega C_{-1}] \qquad [A\text{-}30]$$

$$0 = \frac{\partial^2 C_{p1}}{\partial X^2} - \frac{1}{\Pi_p}[\Pi_{k_1} C_{p1} - \Pi_{k_2}\alpha(C_{+1} + C_{-1}) + i\Omega C_{p1}] \qquad [A\text{-}31]$$

For high salt concentrations and polymer electrolytes with low dielectric constants, $\kappa d \gg 1$, reducing Eq. A-28 to electroneutrality

$$C_{+1} = C_{-1} \qquad [A\text{-}32]$$

Under these conditions, Eq. A-29-A-31 simplify greatly. Adding the equations for cations and anions yields

$$\frac{\partial^2 C_{+1}}{\partial X^2} = (2\alpha\Pi_{k_2} + i\Omega)C_{+1} - \Pi_{k_1} C_{p1} \qquad [A\text{-}33]$$

$$\frac{\partial^2 C_{p1}}{\partial X^2} = \frac{1}{\Pi_p}[-2\alpha\Pi_{k_2} C_{+1} + (i\Omega + \Pi_{k_1})C_{p1}] \qquad [A\text{-}34]$$

From Eq. A-24, A-26, and A-27, we have the dimensionless boundary conditions

$$X = 0: \quad C_{+1} = 0, \quad C_{p1} = 0 \qquad [A\text{-}35]$$

$$X = 1: \quad \frac{\partial C_{+1}}{\partial X} = -\frac{\Pi_I}{2} \qquad [A\text{-}36]$$

$$X = 1: \quad \frac{\partial C_{p1}}{\partial X} = 0 \qquad [A\text{-}37]$$

Solutions for concentration profiles.—Equations A-33 and A-34 can be written in matrix form as

$$\frac{\partial^2}{\partial \underline{X}^2}\underline{C} = \underline{\underline{B}} \cdot \underline{C} \qquad [A\text{-}38]$$

where

$$\underline{\underline{B}} = \begin{bmatrix} i\Omega + 2\alpha\Pi_{k_2} & -\Pi_{k_1} \\ -2\alpha\Pi_{k_2}/\Pi_p & (i\Omega + \Pi_{k_1})/\Pi_p \end{bmatrix} \qquad [A\text{-}39]$$

$$\underline{C} = \begin{bmatrix} C_{+1} \\ C_{p1} \end{bmatrix} \qquad [A\text{-}40]$$

The matrix $\underline{\underline{B}}$ can be decomposed into

$$\underline{\underline{B}} = \underline{\underline{U}}\,\underline{\underline{\Lambda}}\,\underline{\underline{U}}^{-1} \qquad [A\text{-}41]$$

where $\underline{\underline{\Lambda}}$ and $\underline{\underline{U}}$ are defined by

$$\underline{\underline{\Lambda}} = \begin{bmatrix} \Lambda_1 & 0 \\ 0 & \Lambda_2 \end{bmatrix} \qquad [A\text{-}42]$$

$$\underline{\underline{U}} = \begin{bmatrix} u_1 & u_2 \\ 1 & 1 \end{bmatrix} \qquad [A\text{-}43]$$

with eigenvalues

$$\Lambda_1 = \frac{1}{2} i\Omega(1 + 1/\Pi_p) + \frac{1}{2}(\Pi_{k_1}/\Pi_p + 2\alpha\Pi_{k_2}) + \frac{1}{2}\sqrt{-\Omega^2(1 - 1/\Pi_p)^2 + 2i\Omega(2\alpha\Pi_{k_2} - \Pi_{k_1}/\Pi_p)(1 - 1/\Pi_p) + (2\alpha\Pi_{k_2} + \Pi_{k_1}/\Pi_p)^2} \quad [A\text{-}44]$$

$$\Lambda_2 = \frac{1}{2} i\Omega(1 + 1/\Pi_p) + \frac{1}{2}(\Pi_{k_1}/\Pi_p + 2\alpha\Pi_{k_2}) - \frac{1}{2}\sqrt{-\Omega^2(1 - 1/\Pi_p)^2 + 2i\Omega(2\alpha\Pi_{k_2} - \Pi_{k_1}/\Pi_p)(1 - 1/\Pi_p) + (2\alpha\Pi_{k_2} + \Pi_{k_1}/\Pi_p)^2} \quad [A\text{-}45]$$

and eigenvector elements

$$u_1 = \frac{\Pi_p}{4\alpha\Pi_{k_2}}[i\Omega(1/\Pi_p - 1) + (\Pi_{k_1}/\Pi_p - 2\alpha\Pi_{k_2})] - \frac{\Pi_p}{4\alpha\Pi_{k_2}} \times \sqrt{[(i\Omega + \Pi_{k_1})/\Pi_p]^2 + (i\Omega + 2\alpha\Pi_{k_2})^2 + 2\Pi_{k_1}/\Pi_p(2\alpha\Pi_{k_2} - i\Omega) - 2i\Omega/\Pi_p(i\Omega + 2\alpha\Pi_{k_2})} \quad [A\text{-}46]$$

$$u_2 = \frac{\Pi_p}{4\alpha\Pi_{k_2}}[i\Omega(1/\Pi_p - 1) + (\Pi_{k_1}/\Pi_p - 2\alpha\Pi_{k_2})] + \frac{\Pi_p}{4\alpha\Pi_{k_2}} \times \sqrt{[(i\Omega + \Pi_{k_1})/\Pi_p]^2 + (i\Omega + 2\alpha\Pi_{k_2})^2 + 2\Pi_{k_1}/\Pi_p(2\alpha\Pi_{k_2} - i\Omega) - 2i\Omega/\Pi_p(i\Omega + 2\alpha\Pi_{k_2})} \quad [A\text{-}47]$$

The inverse matrix of $\underline{\underline{U}}$ is

$$\underline{\underline{U}}^{-1} = \begin{bmatrix} \frac{1}{u_1 - u_2} & \frac{-u_2}{u_1 - u_2} \\ \frac{-1}{u_1 - u_2} & \frac{u_1}{u_1 - u_2} \end{bmatrix} \quad [A\text{-}48]$$

Thus, Eq. A-39 is converted into

$$\frac{\partial^2}{\partial X^2}\underline{\theta} = \underline{\underline{\Lambda}} \cdot \underline{\theta} \quad [A\text{-}49]$$

with

$$\underline{\theta} = \begin{bmatrix} \theta_+ \\ \theta_p \end{bmatrix} = \underline{\underline{U}}^{-1}\underline{C} \quad [A\text{-}50]$$

The solution to Eq. A-49 is

$$\theta_+ = A_+ \sinh(\sqrt{\Lambda_1}X) + B_+ \cosh(\sqrt{\Lambda_1}X) \quad [A\text{-}51]$$

$$\theta_p = A_p \sinh(\sqrt{\Lambda_2}X) + B_p \cosh(\sqrt{\Lambda_2}X) \quad [A\text{-}52]$$

Since $\underline{C}$ is antisymmetric (Eq. A-35), so is $\underline{\theta}$. We thus have $B_+ = 0$ and $B_p = 0$. The constants A_+ and A_p can be calculated from the other boundary conditions, Eq. A-36 and A-37, expressed via Eq. A-50 as

$$\frac{\partial\theta_+}{\partial X} = -\frac{1}{u_1 - u_2}\frac{\Pi_I}{2} \quad [A\text{-}53]$$

$$\frac{\partial\theta_p}{\partial X} = \frac{1}{u_1 - u_2}\frac{\Pi_I}{2} \quad [A\text{-}54]$$

leading to

$$A_+ = -\frac{1}{u_1 - u_2}\frac{1}{\sqrt{\Lambda_1}\cosh(\sqrt{\Lambda_1})}\frac{\Pi_I}{2} \quad [A\text{-}55]$$

$$A_p = \frac{1}{u_1 - u_2}\frac{1}{\sqrt{\Lambda_2}\cosh(\sqrt{\Lambda_2})}\frac{\Pi_I}{2} \quad [A\text{-}56]$$

Inverting Eq. A-50 provides the concentration profiles

$$C_{+1} = u_1\theta_+ + u_2\theta_p = -\frac{u_1}{u_1 - u_2}\frac{1}{\sqrt{\Lambda_1}\cosh(\sqrt{\Lambda_1})}\frac{\Pi_I}{2}\sinh(\sqrt{\Lambda_1}X) + \frac{u_2}{u_1 - u_2}\frac{1}{\sqrt{\Lambda_2}\cosh(\sqrt{\Lambda_2})}\frac{\Pi_I}{2}\sinh(\sqrt{\Lambda_2}X) \quad [A\text{-}57]$$

$$C_{p1} = \theta_+ + \theta_p = -\frac{1}{u_1 - u_2}\frac{1}{\sqrt{\Lambda_1}\cosh(\sqrt{\Lambda_1})}\frac{\Pi_I}{2}\sinh(\sqrt{\Lambda_1}X) + \frac{1}{u_1 - u_2}\frac{1}{\sqrt{\Lambda_2}\cosh(\sqrt{\Lambda_2})}\frac{\Pi_I}{2}\sinh(\sqrt{\Lambda_2}X) \quad [A\text{-}58]$$

Potential drop across the cell.—Once the concentration profiles are known, the potential drop across the cell can be calculated. From Eq. A-2, the time-dependent component of ion fluxes can be written as

$$N_{+1} = -D_+\frac{\partial c_{+1}}{\partial x} - \frac{D_+F}{RT}c_{+0}\frac{\partial\phi_1}{\partial x} \quad [A\text{-}59]$$

$$N_{-1} = -D_-\frac{\partial c_{-1}}{\partial x} + \frac{D_-F}{RT}c_{-0}\frac{\partial\phi_1}{\partial x} \quad [A\text{-}60]$$

Current density depends on the ionic fluxes according to

$$N_{+1} - N_{-1} = \frac{I_1}{F} \quad [A\text{-}61]$$

After some transformation and the use of electroneutrality, we obtain

$$N_{+1} = -D_s\frac{\partial c_{+1}}{\partial x} + t_+\frac{I_1}{F} \quad [A\text{-}62]$$

$$N_{-1} = -D_s\frac{\partial c_{+1}}{\partial x} - t_-\frac{I_1}{F} \quad [A\text{-}63]$$

$$\frac{\partial\phi_1}{\partial x} = -\frac{RT}{2Fc_{+0}}\left(\frac{N_{+1}}{D_+} - \frac{N_{-1}}{D_-}\right) \quad [A\text{-}64]$$

Substituting Eq. A-62 and A-63 into Eq. A-64 finally yields

$$\frac{\partial\phi_1}{\partial x} = -\frac{RT}{2Fc_{+0}}\left[\frac{D_s(D_+ - D_-)}{D_+D_-}\frac{\partial c_{+1}}{\partial x} + \left(\frac{t_+}{D_+} + \frac{t_-}{D_-}\right)\frac{I_1}{F}\right] \quad [A\text{-}65]$$

or, in dimensionless form

$$\frac{\partial\Phi_1}{\partial X} = -\frac{1}{\alpha}\left[(t_+ - t_-)\frac{\partial C_{+1}}{\partial X} + t_+\Pi_I\right] \quad [A\text{-}66]$$

Integrating Eq. A-66 between the two electrodes gives

$$\Phi_1(1) - \Phi_1(-1) = -\frac{2}{\alpha}[(t_+ - t_-)C_{+1}(1) + t_+\Pi_I] \quad [A\text{-}67]$$

This result is used in Eq. 15 to express the cell potential drop and impedance in terms of C_{+1}.

List of Symbols

A	electrode area, cm^2
c_i	concentration of component i, mol/cm^3
C_i	dimensionless concentration, $C_i \equiv c_i/c_s$
d	cell half-thickness, cm
D_i	diffusion coefficient, cm^2/s
ΔE	potential drop across the cell, V
ΔE_1	potential drop across the cell due to migration, V
ΔE_2	potential drop across the cell due to electrode reaction, V
F	Faraday constant, 96,487 C/mol
I	current density, A/cm^2
k_1	reaction rate constant for salt dissociation, s^{-1}
k_2	reaction rate constant for ion association, cm^3/(mol s)

N_i molar flux, mol/(cm^2 s)
R gas constant, J/(mol K)
R_i reaction rate, mol/(cm^2 s)
t time, s
t_i transference number, $i = +, -$
T temperature, K
u_1, u_2 eigenvector elements defined in Eq. A-44 and A-45
x position, cm
X dimensionless position, $X \equiv x/d$
Z_i valence of species i
Z impedance at frequency ω, Ω
$\overline{Z}$ dimensionless impedance

Greek

α fractional dissociation of salt
ε dielectric permittivity, C^2/(J m)
κ reciprocal Debye length, cm^{-1}
Λ_1, Λ_2 eigenvalues defined in Eq. A-46 and A-47
ν_i reaction coefficient for component i
Π dimensionless groups defined in Table I
Φ dimensionless potential, $\Phi \equiv F\phi/RT$
ϕ potential, V
Ω dimensionless frequency
ω frequency of ac excitation, s^{-1}

Subscripts

$+$ cations
$-$ anions
0 steady-state part of quantity or at zero frequency
1 time-dependent part of quantity
i component, i = +, −, p, s
p ion-pair
s salt
∞ at infinite frequency

Superscripts

σ at an electrode/electrolyte interface

References

1. M. A. Ratner, in *Polymer Electrolyte Reviews*, J. R. MacCallum and C. A. Vincent, Editors, p. 173, Elsevier Applied Science, London (1987).
2. J. R. MacCallum, A. S. Tomlin, and C. A. Vincent, *Eur. Polym. J.*, **22**, 787 (1986).
3. A. Ferry, G. Orädd, and P. Jacobsson, *J. Chem. Phys.*, **108**, 7426 (1998).
4. R. Dupon, B. L. Papke, M. A. Ratner, D. H. Whitmore, and D. F. Shriver, *J. Am. Chem. Soc.*, **104**, 6247 (1982).
5. P. G. Bruce and C. A. Vincent, *Faraday Discuss. Chem. Soc.*, **88**, 43 (1989).
6. C. A. Vincent, *Prog. Solid State Chem.*, **17**, 145 (1987).
7. M. Doyle, T. F. Fuller, and J. Newman, *J. Electrochem. Soc.*, **140**, 1526 (1993).
8. C. Lin, R. E. White, and H. J. Ploehn, *J. Electrochem. Soc.*, **147**, 936 (2000).
9. J. R. MacDonald, *J. Chem. Phys.*, **58**, 4982 (1973).
10. J. R. MacDonald, *J. Chem. Phys.*, **54**, 2026 (1971).
11. J. R. MacDonald, *J. Electroanal. Chem. Interfacial Electrochem.*, **53**, 1 (1974).
12. J. R. MacDonald and D. R. Franceschetti, *J. Chem. Phys.*, **68**, 1614 (1978).
13. R. Pollard and T. Comte, *J. Electrochem. Soc.*, **136**, 3734 (1989).
14. J. W. Lorimer, *J. Power Sources*, **26**, 491 (1989).
15. D. R. Franceschetti, J. R. MacDonald, and R. P. Buck, *J. Electrochem. Soc.*, **138**, 1368 (1991).
16. J. Newman, *Electrochemical Systems*, 2nd ed., Prentice-Hall, Englewood Cliffs, NJ (1991).
17. J. C. Slattery, *Advanced Transport Phenomena*, Oxford University Press, Oxford, U.K. (1999).
18. P. Ferloni, G. Chiodelli, A. Magistris, and M. Sanesi, *Solid State Ionics*, **18&19**, 265 (1986).
19. W. Gorecki, R. Andreani, C. Berthier, M. Armand, M. Mali, J. Roos, and D. Brinkmann, *Solid State Ionics*, **18&19**, 295 (1986).